Acta Cryst. (1974). B30, 365

The Conformation of *N*-Acetyl-α-D-muramic Acid and its Relationship to Penicillin

BY J. R. KNOX AND N. S. MURTHY

Biological Sciences Group and Institute of Materials Science, University of Connecticut, Storrs, Connecticut 06268, *U.S.A.*

(*Received* 28 *August* 1973; *accepted* 9 *October* 1973)

N-Acetyl-α-D-muramic acid monohydrate, $C_{11}H_{19}NO_8.H_2O$, crystallizes in space group $P2_12_12_1$ with $a=7{\cdot}833\pm0{\cdot}005$, $b=8{\cdot}084\pm0{\cdot}005$, $c=23{\cdot}495\pm0{\cdot}018$ Å and $Z=4$. The structure was solved by direct methods and refined by least-squares calculations to $R=0{\cdot}079$ for 1060 observed reflections. The molecule has the $^4C_1$ conformation with internal torsion angles ranging from 49 to 62°. The C(1)–O(1)H bond ($1{\cdot}38\pm0{\cdot}01$ Å) is significantly shorter than the mean of four other single bonds. Ring C–O distances are 1·42 and $1{\cdot}45\pm0{\cdot}01$ Å for C(1)–O(5) and C(5)–O(5), respectively. An intramolecular hydrogen bond of 2·96 Å exists between the *N*-acetyl amide and the lactyl carbonyl. The resulting molecular conformation is unlike that proposed in earlier model studies which pointed to a similarity between penicillin and *N*-acetyl muramic acid as the basis for the activity of the antiboitic.

Introduction

Penicillin and cephalosporin antibiotics stop bacterial growth by being mistaken for certain cell wall precursors by the enzymes which synthesize the wall network. These enzymes either use penicillin to form a weak wall, or are inactivated by becoming irreversibly bound to the antibiotic (Strominger, Izaki, Matsuhashi & Tipper, 1967). Exactly which precursor is resembled by penicillin has been the subject of biochemical studies by several groups. Collins & Richmond (1962) suggested, on the basis of model building, a topographic similarity of penicillin to *N*-acetyl-α-muramic acid (NAM, shown below in Haworth projection).

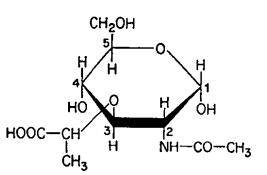

This compound was suggested by these authors and by others (Felsenfeld & Handschumacher, 1967) because it is one of the two glucopyranose components in the cell wall polysaccharide $(-NAM-NAG-)_n$, where NAG is *N*-acetylglucosamine. These β(1–4) polysaccharide chains are cross-linked through NAM by short polypeptides to complete the two-dimensional wall network, and other authors believe it is rather at this later stage of wall synthesis that penicillin is antibiotic. For example, Wise & Park (1965) use molecular models to show a structural relationship between penicillin and the L-alanyl-γ-D-glutamyl portion of the peptide cross-link. On the other hand, Tipper & Strominger (1965) and recently Lee (1971) provide evidence which strongly points to *x*-D-alanyl-D-alanine as the precursor most like penicillin. To test these hypotheses we report now the molecular structure of NAM and compare its topography with benzylpenicillin (Pitt, 1952). We plan to analyze derivatives of the other two dipeptides.

Active interest in the chair to half-chair transition of NAM exists in studies on the mechanism of lysozyme (Phillips, 1967), an enzyme which ruptures cell wall by breaking the glycosidic linkage between NAM and NAG. Now that the active site geometry of the enzyme has been established (Blake, Johnson, Mair, North, Phillips & Sarma, 1967), future substrate binding studies will require conformational and structural details of the NAM molecule.

Experimental

N-Acetylmuramic acid (3-*O*-D-α-carboxyethyl-*N*-acetyl-D-glucosamine, NAM) was obtained from Sigma Chemical Company and was crystallized as the monohydrate by slow evaporation of ethanol–water solutions at room temperature. The space group and lattice parameters were determined from precession photographs. Unit-cell constants were refined from a least-squares fitting of diffractometer angles for 12 centered reflections.

Crystal data

$C_{11}H_{19}NO_8.H_2O$, F.W. 311·2, $F(000)=664$.
Orthorhombic.
$a=7{\cdot}833\pm0{\cdot}005$ Å,
$b=8{\cdot}084\pm0{\cdot}005$,
$c=23{\cdot}495\pm0{\cdot}018$,
$D_x=1{\cdot}389$ g cm^{-3} for $Z=4$, $D_m=1{\cdot}38\pm0{\cdot}02$ g cm^{-3} by flotation in carbon tetrachloride–xylene.
Linear absorption coefficient (Mo $K\alpha$) $\mu=1{\cdot}25$ cm^{-1}.
Systematic extinctions: $h00$ for h odd, $0k0$ for k odd, $00l$ for l odd. Space group $P2_12_12_1$ (D_2^4, No. 19).

A crystal measuring $0{\cdot}3\times0{\cdot}5\times0{\cdot}9$ mm was sealed in a glass capillary. Intensity data were collected with Mo $K\alpha$ radiation on a Picker Corporation FACS-I

four-circle diffractometer equipped with a graphite monochromator. A 1° min^{-1} 2θ scan was used with stationary 20 s background counts on either side of the nominal 2° scan. Three standard reflections were monitored every 100 reflections. Of the 1548 unique reflections measured to 50° 2θ, 485 reflections had background-corrected intensities I_o less than $3\sigma(I_o)$ and were assigned an intensity of $I_o+3\sigma(I_o)$. The standard error σ is estimated as $[CN+BG+p^2I_0^2]^{1/2}$ where CN is the peak count, BG is the total background count, and p is an arbitrary stability factor taken as 5%. Corrections were made for Lorentz–polarization effects, but not for absorption. Fourier and least-squares calculations were done with X-RAY System (1972) on an IBM 360 computer. Scattering curves were taken from *International Tables for X-ray Crystallography* (1968).

Structure determination and refinement

The 1063 observed reflections were converted to normalized $|E|$ values by means of a K curve, and the symbolic addition procedure for non-centrosymmetric crystals was applied (Karle & Karle, 1966). Phases used for origin and enantiomorph assignment are shown in Table 1 together with three symbolic phases.

Table 1. *Starting phase assignments*

h	k	l	$\|E\|$	ψ
4	0	15	3·07	$\pi/2$
0	7	6	2·45	$-\pi/2$
7	0	8	1·99	0
4	8	7	2·50	$\pi/2$
0	2	9	2·20	a
3	1	9	2·25	b
1	3	8	2·65	c

In addition, phases of four structure invariants which were determined using the $\sum_1$ formula (Hauptman & Karle, 1953) are shown in Table 2. Only the latter two phases were used with the starting phases in Table 1. To implement the phasing procedure, the three symbolic phases were systematically assigned numeric values in increments of $\pi/4$ radians. The multiple-solution tangent formula procedure developed by Drew, Templeton & Zalkin (1969) was used. After 30 cycles of tangent-formula refinement, including in three stages the 180 reflections with $|E|\geq 1{\cdot}45$, the phase set with an R(Karle) index equal to 0·21 was used to calculate an E map which revealed all 20 non-hydrogen atoms in the molecule and one water oxygen atom. The initial R value $\sum||F_o|-|F_c||/\sum|F_o|$ based on E map coordinates was 26·1% for observed reflections.

Table 2. *An application of the* $\sum_1$ *formula*

h	k	l	$\|E\|$	$P+$	ψ(predicted)	ψ(final)
0	8	10	2·39	0·65	0	0
0	2	8	2·20	0·66	0	0
2	6	0	2·05	0·11	π	π
0	6	16	1·71	0·81	0	0

In the full-matrix least-squares refinement the quantity minimized was $\sum w(|F_o|-|F_c|)^2$, where $w=\sigma^{-2}(F_o)$. After six cycles of refinement with isotropic temperature factors, parameter shifts became less than their standard deviations and the R index was 14·7%. At this stage six hydrogen atoms were located in difference Fourier maps. Seven additional cycles of refinement with anisotropic temperature factors for non-hydrogen atoms gave an R index of 7·9%, at which point all parameter shifts were less than $0{\cdot}2\sigma$. Positional and isotropic thermal factors (of parent atom) for hydrogen atoms were not varied. Water hydrogens could not be

Table 3. *Fractional coordinates* ($\times 10^4$) *and anisotropic temperature factor coefficients* ($\times 10^3$)

The expression used is $T=\exp[-2\pi^2(a^{*2}U_{11}h^2+b^{*2}U_{22}k^2+c^{*2}U_{33}l^2+2a^*b^*hkU_{12}+2a^*c^*U_{13}hl+2b^*c^*U_{23}kl)]$. Standard deviations are given in parentheses.

	x	y	z	U_{11}	U_{22}	U_{33}	U_{12}	U_{13}	U_{23}
C(1)	1582 (12)	−524 (10)	4375 (3)	59 (7)	33 (7)	26 (4)	−19 (5)	−7 (4)	4 (4)
C(2)	3076 (11)	30 (9)	3991 (3)	42 (6)	23 (4)	26 (4)	−3 (4)	1 (4)	5 (4)
C(3)	2472 (11)	1517 (9)	3639 (3)	54 (6)	15 (4)	29 (4)	1 (4)	13 (4)	4 (3)
C(4)	936 (12)	1014 (10)	3290 (3)	52 (6)	28 (4)	30 (4)	0 (4)	−11 (4)	1 (4)
C(5)	−471 (13)	257 (10)	3652 (4)	48 (6)	33 (4)	33 (4)	−7 (5)	−4 (5)	−4 (4)
C(6)	−1854 (13)	−623 (11)	3330 (4)	49 (6)	44 (5)	52 (5)	1 (5)	−4 (5)	−18 (5)
C(7)	5505 (12)	−634 (9)	4611 (3)	47 (6)	23 (4)	35 (4)	3 (5)	−6 (5)	1 (4)
C(8)	6807 (14)	−8 (11)	4991 (4)	55 (6)	35 (5)	62 (6)	−2 (5)	−14 (6)	3 (5)
C(9)	4103 (11)	3699 (9)	3170 (3)	45 (5)	15 (4)	37 (4)	−13 (4)	6 (4)	11 (3)
C(10)	4624 (12)	4619 (8)	3713 (4)	46 (5)	11 (3)	43 (5)	11 (4)	−10 (5)	2 (4)
C(11)	5427 (14)	3838 (11)	2724 (3)	80 (7)	39 (5)	39 (5)	−19 (6)	8 (6)	12 (4)
O(1)	1172 (9)	767 (8)	4733 (2)	78 (5)	53 (4)	30 (3)	−15 (4)	13 (3)	−6 (3)
O(3)	3898 (8)	1958 (6)	3284 (2)	53 (4)	9 (2)	32 (3)	−1 (3)	10 (3)	−3 (2)
O(4)	163 (8)	2452 (7)	3038 (2)	57 (4)	36 (3)	44 (3)	3 (4)	−9 (3)	14 (3)
O(5)	207 (8)	−1022 (6)	4024 (2)	53 (4)	25 (3)	46 (3)	−15 (3)	−1 (3)	8 (3)
O(6)	−1236 (10)	−1987 (8)	3019 (3)	91 (6)	42 (4)	52 (4)	−17 (4)	3 (4)	−15 (4)
O(7)	5305 (9)	−2163 (6)	4544 (2)	81 (5)	15 (3)	47 (3)	−4 (3)	−22 (4)	3 (3)
O(10)	5201 (10)	3989 (7)	4120 (2)	93 (5)	22 (3)	39 (3)	5 (4)	−17 (4)	−2 (3)
O(12)	4374 (10)	6206 (6)	3655 (2)	108 (6)	16 (3)	47 (4)	3 (4)	−24 (4)	−6 (3)
N(2)	4531 (10)	444 (8)	4336 (3)	45 (5)	23 (4)	35 (4)	−8 (4)	−6 (4)	9 (3)
O(*W*)	844 (15)	184 (10)	1310 (4)	121 (8)	54 (5)	138 (7)	−2 (6)	−8 (8)	25 (6)

located, and the amide and methyl hydrogens had to be placed in most likely positions. Unobserved reflections were omitted from the refinement, as were the three reflections 101, 017, and 039 which had $wAF > 15$ electrons. The final difference map contained only random background of $\pm 0{\cdot}3$ eÅ^{-3}. The final atomic coordinates [D configuration at C(5)] and temperature factors are given in Tables 3 and 4, and observed and calculated structure factors (excluding water hydrogens) are shown in Table 5.

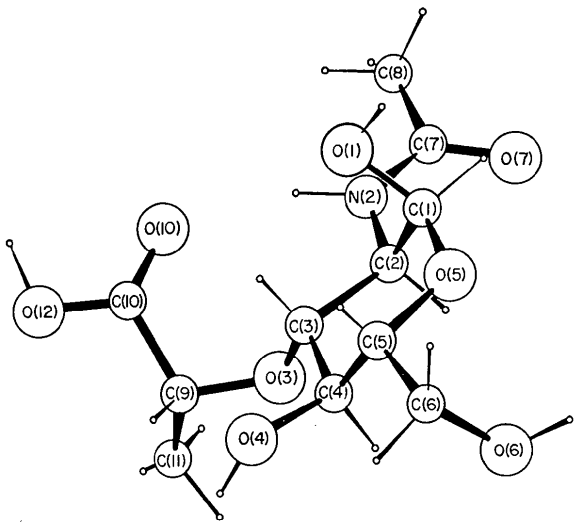

Fig. 1. Conformation of *N*-acetyl-α-D-muramic acid.

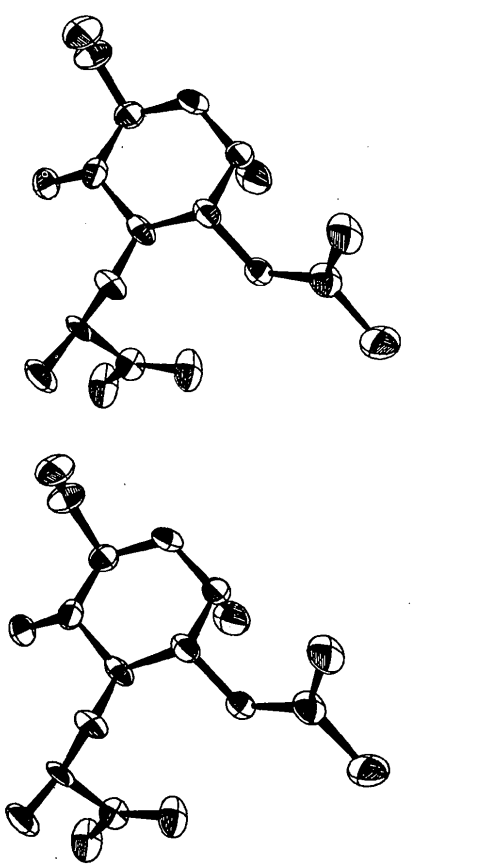

Fig. 2. Stereoscopic view of molecule. The ellipsoids are drawn at the 50% probability level using a program of Johnson (1965). Hydrogen atoms are not shown.

Table 4. *Fractional coordinates* ($\times 10^3$) *of hydrogen atoms and isotropic temperature factor coefficients* ($\times 10^3$)

$T = \exp(-8\pi^2 U \sin^2\theta/\lambda^2)$.

	x	y	z	U
H(C1)	217	840	465	33
H(C2)	333	907	370	30
H(C3)	210	230	393	26
H(C4)	143	27	295	36
H(C5)	97	597	111	38
H1(C6)	283	433	130	33
H2(C6)	240	527	200	33
H1(C8)	160	517	470	38
H2(C8)	233	467	7	38
H3(C8)	200	377	500	38
H(C9)	287	417	306	29
H1(C11)	387	833	210	43
H2(C11)	410	960	239	43
H3(C11)	507	800	260	43
H(O12)	510	673	404	49
H(O1)	63	17	501	44
H(O4)	27	300	267	46
H(O6)	127	233	178	52
H(N2)	483	150	425	27

Discussion

The molecule, and the atom numbering scheme used here, are shown in Fig. 1; a stereoview is given in Fig. 2.

Glucopyranose ring

The glucopyranose ring has the chair ($^4C_1$) conformation. Torsion angles involving the ring atoms are given in Table 6 and are compared with those calculated by us for the related molecule *N*-acetyl-α-D-glucosamine: NAG (Johnson, 1966). Torsion angles range from 49·5 to 62·0° in NAM and from 53·3 to 63·8° in NAG. A smaller range of 55·8 to 61·7° is expected for an 'ideal' sugar ring (Kim & Jeffrey, 1967). The rather small C(4)–C(5) torsion angle in NAM is the result of either the participation of the hydroxyl groups on C(4) and C(6) in strong hydrogen bonding or the accommodation of the ring to stresses resulting from an internal hydrogen bond between acetyl and lactyl groups. Torsion angles on the C(4)C(5) half of the NAM chair are generally somewhat smaller than the corresponding angles on the C(1)C(2) half. Nevertheless, the coordinates of the six ring atoms are within 0·10 Å of the standard coordinates proposed by Ramachandran, Ramakrishnan & Sasisekharan (1963) for a pyranose ring (Table 7).

Bond distances and angles in the ring are given in Table 8. None of the four C–C bonds in NAM differs significantly from the mean value of 1·527 ± 0·012 Å,

Table 5. *Observed and calculated structure factors* (× 10)

Reflections marked * were omitted from refinement.

Table 6. *A comparison of selected torsion angles in the N-acetyl derivatives of muramic acid and glucosamine (Johnson, 1966)*

Zero angle is defined with front and rear bond superposed in projection down middle bond. Angle is positve if right-handed rotation of either front or rear bond is required for their superposition.

Atoms	Torsion angle	
	NAM	NAG
O(5)C(1)–C(2)C(3)	62·0°	53·3°
C(1)C(2)–C(3)C(4)	−59·0	−59·0
C(2)C(3)–C(4)C(5)	53·7	63·3
C(3)C(4)–C(5)O(5)	−49·5	−63·0
C(4)C(5)–O(5)C(1)	54·5	63·8
C(5)O(5)–C(1)C(2)	−61·1	−58·6
N(2)C(2)–C(1)O(1)	60·4	55·3
N(2)C(2)–C(3)O(3)	60·4	67·3
O(3)C(3)–C(4)O(4)	−74·3	−67·1
O(4)C(4)–C(5)C(6)	74·3	67·8
O(5)C(5)–C(6)O(6)	−59·1	−61·2
C(3)C(2)–N(2)C(7)	−168·3	−100·5
C(2)N(2)–C(7)O(7)	6·9	−27·0
C(2)C(3)–O(3)C(9)	−145·7	–
C(3)O(3)–C(9)C(10)	68·6	–
O(3)C(9)–C(10)O(10)	18·2	–

Table 7. *Transformed coordinates* (Å) *of ring atoms in N-acetylmuramic acid compared with standard coordinates (in parentheses) of Ramachandran et al.* (1963)

The origin is at C(3), X is along C(3)–C(5), Y is in the plane of C(1)C(3)C(5), and Z is normal to XY plane in a right-handed system. Estimated errors are 0·01 Å and 0·04 Å for NAM and standard coordinates, respectively.

C(1)	1·326 (1·34)	2·108 (2·08)	0·000 (0·00)
C(2)	0·064 (0·05)	1·422 (1·44)	−0·568 (−0·47)
C(3)	0·000 (0·00)	0·000 (0·00)	0·000 (0·00)
C(4)	1·255 (1·24)	−0·746 (−0·76)	−0·395 (−0·42)
C(5)	2·521 (2·50)	0·000 (0·00)	0·000 (0·00)
O(5)	2·464 (2·45)	1·386 (1·33)	−0·435 (−0·48)

which is equal to the mean in NAG and other sugars (Kim & Jeffery, 1967). Equality of ring C–O distances is expected in monosaccharides, though significant differences are common in γ-lactones and in glycosides in which the C(1)–O(1) bond is axial (Berman, Chu & Jeffrey, 1967). In NAM the two ring C–O bonds differ by 0·04 Å, but deviate from their mean by only 1·8σ. The shorter bond is adjacent to the anomeric carbon C(1), as is the case in many glycosides.

Table 8. *Distances* (Å) ($\sigma \times 10^3$) *and angles* (°) ($\sigma \times 10$) *in N-acetyl-α-D-muramic acid with standard deviations in parentheses*

Bond lengths

C(1)–C(2)	1·543 (12)	C(1)—O(1)	1·379 (10)
C(2)–C(3)	1·533 (11)	C(1)—O(5)	1·417 (11)
C(3)–C(4)	1·513 (12)	C(5)—O(5)	1·453 (10)
C(4)–C(5)	1·520 (13)	C(3)—O(3)	1·438 (10)
C(5)–C(6)	1·503 (14)	C(4)—O(4)	1·438 (10)
C(7)–C(8)	1·448 (13)	C(6)—O(6)	1·409 (11)
C(9)–C(10)	1·532 (11)	C(7)—O(7)	1·256 (9)
C(9)–C(11)	1·478 (13)	C(9)—O(3)	1·440 (9)
C(2)–N(2)	1·439 (11)	C(10)–O(10)	1·175 (10)
N(2)–C(7)	1·328 (11)	C(10)–O(12)	1·305 (9)

Table 8 (*cont.*)

Valence angles

O(5)—C(1)—C(2)	108·5 (6)	C(2)–N(2)–C(7)	125·3 (7)
C(1)—C(2)—C(3)	107·9 (7)	C(8)–C(7)–N(2)	118·5 (7)
C(2)—C(3)—C(4)	109·1 (6)	C(8)–C(7)–O(7)	120·7 (8)
C(3)—C(4)—C(5)	112·4 (7)	N(2)–C(7)–O(7)	120·8 (8)
C(4)—C(5)—O(5)	110·9 (8)		
C(5)—O(5)—C(1)	115·2 (6)		
		O(5)–C(1)–O(1)	113·2 (8)
C(3)—O(3)—C(9)	115·7 (6)	O(1)–C(1)–C(2)	108·3 (7)
O(3)—C(9)—C(11)	106·4 (6)	C(1)–C(2)–N(2)	109·7 (6)
O(3)—C(9)—C(10)	110·5 (6)	N(2)–C(2)–C(3)	111·5 (6)
C(11)–C(9)—C(10)	111·5 (7)	C(2)–C(3)–O(3)	105·4 (7)
C(9)—C(10)–O(10)	124·8 (7)	C(4)–C(3)–O(3)	111·6 (6)
C(9)—C(10)–O(12)	110·7 (7)	C(3)–C(4)–O(4)	110·0 (6)
O(10)–C(10)–O(12)	124·5 (7)	O(4)–C(4)–C(5)	104·4 (7)
		C(4)–C(5)–C(6)	115·4 (7)
		C(6)–C(5)–O(5)	103·3 (7)
		C(5)–C(6)–O(6)	112·6 (8)

Hydrogen-bond distances and angles with symmetry code

(i)	x	y	z	(iv)	$-x$	$\frac{1}{2}+y$	$\frac{1}{2}-z$
(ii)	x	$-1+y$	z	(v)	$-x$	$-\frac{1}{2}+y$	$\frac{1}{2}-z$
(iii)	$-\frac{1}{2}+x$	$\frac{1}{2}-y$	$1-z$				

A H O	A–H	H–O	A–O	∠A–H–O
N(2)——H···O(10^{i})	0·91 Å	2·06 Å	2·96 Å	172°
O(7)····H—O(12^{ii})	1·49	1·15	2·58	154
O(1)——H···O(10^{iii})	0·91	2·18	2·81	125
O(4)——H···O(6^{iv})	0·97	1·79	2·66	147
O(W)·····O(4^{v})	–	–	2·80	–
O(W)···H—O(6^{iv})	2·09	0·72	2·79	166

Valence angles at the carbon atoms in the ring range from 107·9 to 112·4° with a mean of 109·8°. The angle at the ring oxygen O(5) is 115·2°, being 1–2° higher than in other glycopyranoses (Ramachandran, Ramakrishna & Sasisekharan, 1963; Jeffrey & Rosenstein, 1964), but it is equal to the angle at the O(3) ether linkage. The relative flattening of the C(4)C(5)O(5) side of the ring, as reflected in the valence angles, derives from the hydrogen bonding mentioned above which decreases the C(4)–C(5) torsion angle.

Ring substituents

The molecule observed here is the α anomer. Coexistence in the crystal of some β molecules is possible if mutarotation had occurred in solution prior to crystallization. In the final Fourier difference map the residual density near the equatorial position of C(1) was no higher than other background peaks.

Berman, Chu & Jeffrey (1967), in a study of anomeric bond character in free sugars, concluded that anomeric bonds are often shortened by about 0·04 Å, and that in the case of *glycosides* with axial anomeric bonds, differences in ring C–O distances will appear instead of significant anomeric shortening. In NAM, the anomeric bond length is 1·38 Å and is in fact shorter by 5σ than the 1·43 Å mean of the four other non-ring C–O distances, excluding carboxyl and carbonyl distances. The case of NAM is then unusual in that the short C(1)–O(1) bond occurs in conjunction with a near inequality of ring C–O bond lengths.

The bulky substituents at the C(2) and C(3) positions, as well as the HO(4) hydroxyl and HO(6) alcohol, occupy uncrowded equatorial positions. Torsion angles between bonds to the first atom of each group are given in Table 6. The *gauche* configuration prevails around the outside of the ring, with HO(4) involved in torsions somewhat larger than 60° because of intermolecular hydrogen bonding.

The *trans* peptide link in the *N*-acetyl group deviates slightly from planarity by a 7° rotation about the N(2)–C(7) bond. The non-hydrogen atoms in the group, including C(2), are within 0·05 Å of the best least-squares plane. The r.m.s. displacement is 0·03 Å. The considerable inclination of the *N*-acetyl plane (51°) with respect to the best plane of all six ring atoms results from *intra*molecular hydrogen bonding. In NAG, where no internal hydrogen bonding exists, the *N*-acetyl plane is more nearly perpendicular (78°) to the ring plane, and the amide NH bonds to the amide carbonyl on a neighboring molecule. Bond lengths and angles in the peptide group are within 0·02 Å and 3° of standard values (Marsh & Donohue, 1967). The C(7)–CH_3 bond is 0·06 Å shorter, by about 4σ, than usual distances. This shortening is not likely to be real, and may be due to the thermal or librational motion far from the molecular center.

An intramolecular hydrogen bond exists between the *N*-acetyl and lactyl groups. The planar *N*-acetyl group is turned 168° about the C(2)–N(2) bond to a position *trans* to C(3). In this position, the N–H bond is able to form the hydrogen bond (2·96 Å) with the carbonyl oxygen atom O(10) of the lactyl group. The bond is formed in spite of the fact that the carbonyl oxygen atom must come very near (2·76 Å) the ether oxygen O(3). Consequently minor angular distortions appear at the carboxyl carbon C(10), so that the C–C–O angle *cis* to O(3) is larger, and the angle *trans* is smaller, than normal values (Marsh & Donohue, 1967). The 115·7° ether angle is unaffected by this repulsion, being perpendicular to it, and it is equal to the ether angle in the ring. The two ether distances C–O(3) are equivalent. The configuration of the asymmetric carbon C(9) in the lactyl group is D, with the D configuration for C(5). This finding confirms an earlier C(9) assignment based on a chemical study of NAM (Strange & Kent, 1959).

The alcohol oxygen O(6) is *gauche* to the ring oxygen O(5), and the corresponding torsion angle along the C(5)–C(6) bond is 59°. Bond distances in the group are normal, and the valence angle at C(6) is 112·6°.

Comparison with penicillin

Collins & Richmond (1962), in their comparison of CPK models of NAM and benzylpenicillin, showed that three oxygen atoms in NAM, *viz.* O(3), O(7) and O(10), could have the same relative positions as two oxygen atoms and the lactam nitrogen atom of penicillin (Fig. 3). To show the molecule-to-molecule relationship, they had to build into their NAM model a highly non-planar peptide linkage having the carbonyl bond perpendicular to the amide bond. In their model the lactyl methyl group is rotated extremely close to the axial hydrogen atom on C(3). Their statement that this particular NAM conformation is not the most stable is confirmed by our finding of a considerably less-crowded conformation, described above.

Differences between their model and the observed structure, except for the anomeric OH position, are primarily in the torsion angles about N(2)–C(2), O(3)–C(9), and C(9)–C(10), all of which differ by at least 90° from the observed torsion angles. Further, it is noteworthy that these side group conformations are stabilized by an internal hydrogen bond between the adjacent *N*-acetyl and lactyl groups. Were this bond not important, external hydrogen bonding interactions would be expected as, for example, in the NAG structure (Johnson, 1966); NAG has no lactyl substituents, but the NH in question bonds instead to C=O groups on neighboring molecules. N.m.r. studies are planned to see if the NAM hydrogen bond exists in solution. Even if the bond is weakened in an aqueous environment, other changes must occur in NAM for it to resemble penicillin: a rotation of the lactyl group to the crowded position of Collins & Richmond's model, and a severe 90° out-of-plane twist in the *N*-acetyl peptide linkage. It may be argued that an enzyme on the growing cell wall could bring about these changes in NAM, in which case the distorted conformation of Collins & Richmond (1962) could be a *transition-state* conformation. Lee (1971) uses a similar approach in describing penicillin as an analog of *x*-D-alanyl-D-alanine (see *Introduction*). Our results show that, while penicillin may bear some resemblance to a high-energy transition-state conformation of NAM, there is little resemblance with the low-energy conformation observed by us in the hydrated crystal.

Hydrogen bonding and molecular packing

In addition to the intramolecular O(10)···HN(2) bond discussed previously, there exist eight intermolecular oxygen–oxygen interactions per molecule (Fig. 4 and Table 8). All oxygen atoms of the sugar, except the ether oxygens, are involved in at least one interaction < 3·0 Å in length. Strong hydrogen bonds (2·58 Å) from the lactyl OH to the *N*-acetyl C=O link the molecules in a row along **b**. The water molecule assists this alignment by bridging between HO(4) and HO(6) at 2·8 Å. In the **c** direction moderately strong bonds (2·66 Å), again involving HO(4) and HO(6), cross-link the molecular rows side-by-side. This cross-linking is strengthened by a 2·8 Å bond from the anomeric O(1) hydrogen to a lactyl carbonyl group CO(10).

Most hydrogen bonds lie in planes generally perpendicular to the *a* axis. Each molecule bridges between two planes of hydrogen bonds: one plane contains the bond O(1)H···O(10) and the bonds between HO(4), HO(6), and water, and the other plane contains the bond O(10)···HO(1) and the bonds between

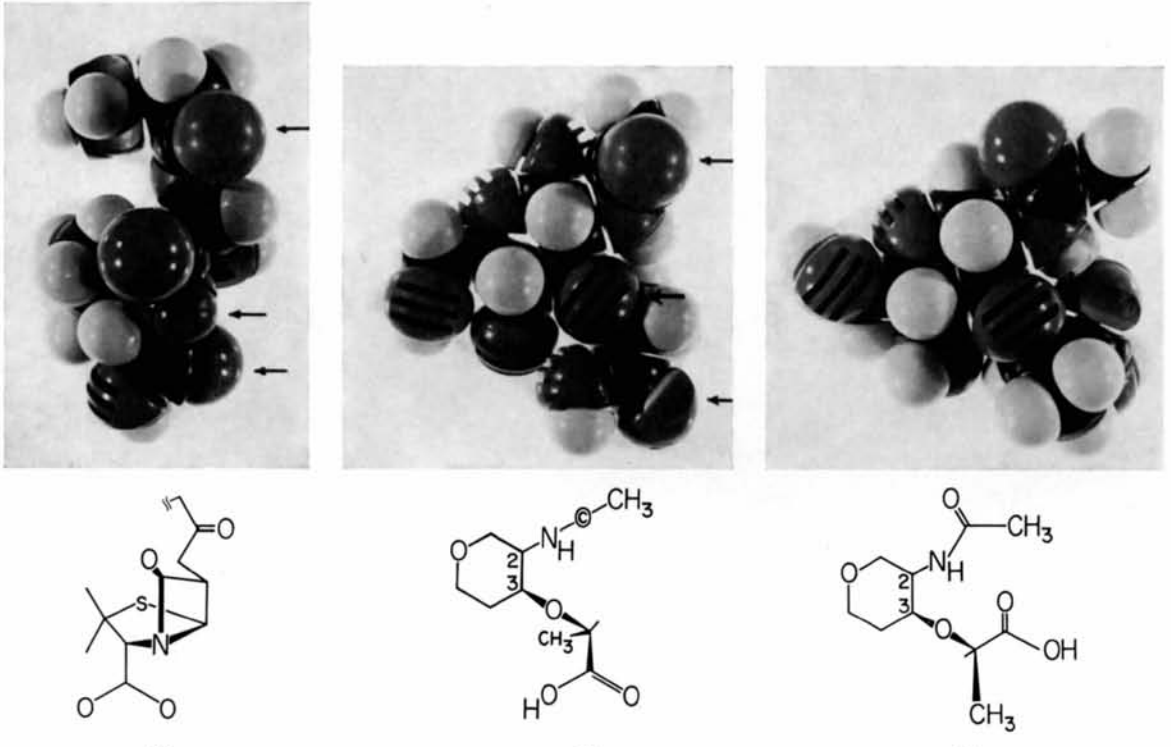

Fig. 3. CPK solid models of (*a*) benzylpenicillin (Pitt, 1952), (*b*) *N*-acetylmuramic acid as proposed by Collins & Richmond (1962), and (*c*) *N*-acetylmuramic acid as observed in this study. Schematics of each model are also shown. Arrows indicate oxygen and nitrogen atoms discussed in text.

[*To face p.* 370]

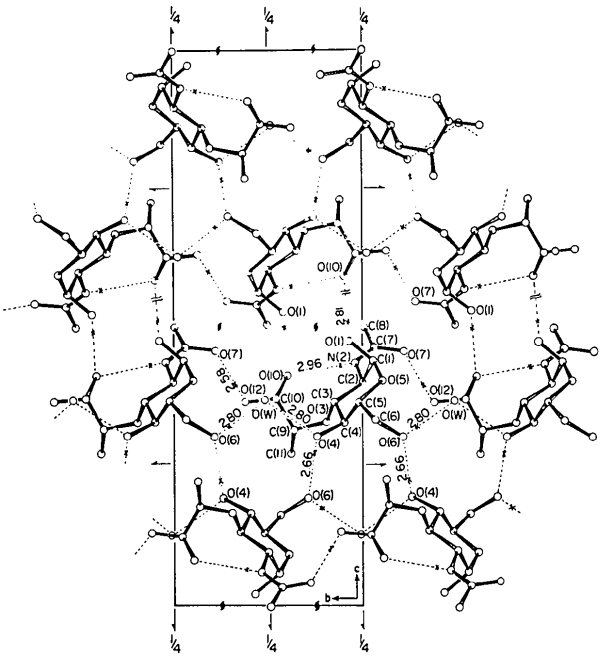

Fig. 4. Crystal structure and hydrogen bonding.

O(7) and HO(12). This scheme places the pyranose ring almost perpendicular to these hydrogen bond planes. The sugar–sugar interactions are stronger than sugar–water interactions. The water molecule is held in position between sugar molecules by only two moderately strong bonds to HO(4) and HO(6).

Hydrogen-bonded helices are a common feature in several carbohydrate structures (Chu & Jeffrey, 1967), and they are present in NAM also. The bonds O(4)H···O(6) → O(6)H···O(*W*) → O(*W*)H···O(4) → O(4)H···O(6) form a tight spiral around the unit-cell screw axis at $x=0$, $z=\frac{1}{4}$ and at $x=\frac{1}{2}$, $z=\frac{3}{4}$ with six bonds per turn. These spirals extend through the crystal parallel to the *b* axis. The first spiral is right-handed whereas the one at $z=\frac{3}{4}$ is left-handed.

We thank M. Hubbard and L. Diaz for preparing the figures. This work was supported by Grant AI-10925 from the National Institutes of Health. Computations were done at the University of Connecticut Computer Center.

References

BERMAN, H. M., CHU, S. S. C. & JEFFREY, G. A. (1967). *Science*, **157**, 1576–1577.

BLAKE, C. C. F., JOHNSON, L. N., MAIR, G. A., NORTH, A. C. T., PHILLIPS, D. C. & SARMA, V. R. (1967). *Proc. Roy. Soc.* B**167**, 378–388.

CHU, S. S. C. & JEFFREY, G. A. (1967). *Acta Cryst.* **23**, 1038–1049.

COLLINS, J. F. & RICHMOND, M. H. (1962). *Nature, Lond.* **195**, 142–143.

DREW, M. G. B., TEMPLETON, D. H. & ZALKIN, A. (1969). *Acta Cryst.* B**25**, 261–267.

FELSENFELD, H. & HANDSCHUMACHER, R. E. (1967). *Mol. Pharmacol.* **3**, 153–160.

HAUPTMAN, H. & KARLE, J. (1953). *Solution of the Phase Problem. I. The Centrosymmetrical Crystal.* Ann Arbor: Edwards Brothers, Inc.

International Tables for X-ray Crystallography (1968). Vol. III, 2nd ed., pp. 202–207. Birmingham: Kynoch Press.

JEFFREY, G. A. & ROSENSTEIN, R. D. (1964). *Advanc. Carbohydr. Chem.* **19**, 7–22.

JOHNSON, C. K. (1965). *ORTEP*. Report ORNL-3794, Oak Ridge National Laboratory, Oak Ridge, Tennessee.

JOHNSON, L. N. (1966). *Acta Cryst.* **21**, 885–891.

KARLE, J. & KARLE, I. L. (1966). *Acta Cryst.* **21**, 849–859.

KIM, S. H. & JEFFREY, G. A. (1967). *Acta Cryst.* **22**, 537–545.

LEE, B. (1971). *J. Mol. Biol.* **61**, 463–469.

MARSH, R. E. & DONOHUE, J. (1967). *Advanc. Protein Chem.* **22**, 235–256.

PHILLIPS, D. C. (1967). *Proc. Natl. Acad. Sci. U.S.* **57**, 484–495.

PITT, G. J. (1952). *Acta Cryst.* **5**, 770–775.

RAMACHANDRAN, G. N., RAMAKRISHNAN, D. & SASISEKHARAN, V. (1963). *Aspects of Protein Structure*, p. 121. New York and London: Academic Press.

STRANGE, R. E. & KENT, L. H. (1959). *Biochem. J.* **71**, 333–339.

STROMINGER, J. L., IZAKI, K., MATSUHASHI, M. & TIPPER, D. L. (1967). *Federation Proc.* **26**, 9–21.

TIPPER, D. J. & STROMINGER, J. L. (1965). *Proc. Natl. Acad. Sci. U.S.* **54**, 1133–1141.

WISE, E. M. & PARK, J. T. (1965). *Proc. Natl. Acad. Sci. U.S.* **54**, 75–81.

X-RAY System (1972). Technical report TR-192 of the Computer Center, Univ. of Maryland, June 1972.